ORGANOMETALLICS

pubs.acs.org/Organometallics Article

Experimental and Computational Studies of Phosphine Ligand Displacement in Iridium−Pincer Complexes Employing Pyridine or Acetonitrile

Sara Shafiei-Haghighi, Aneelman Brar, Daniel K. Unruh, Anthony F. Cozzolino,* and Michael Findlater*

Cite This: https://dx.doi.org/10.1021/acs.organomet.0c00202 Read Online

ACCESS | Metrics & More | Article Recommendations | Supporting Information

ABSTRACT: This report describes the synthesis, characterization, and ligand exchange studies of iridium-based, pincer complexes. (^{tBu}POCOP)Ir(PPh$_3$) (^{tBu}POCOP = 2,6-bis(di-*tert*-butylphosphonito)benzene) serves as a convenient source of the latent Ir(I), 14-electron species [(^{tBu}POCOP)Ir] and is susceptible to ligand exchange chemistry; reactions with acetonitrile and pyridine afford the corresponding (^{tBu}POCOP)Ir(NCMe) (**2**) and (^{tBu}POCOP)Ir(Py) (**3**) complexes, respectively. Varying concentrations of both pyridine and acetonitrile, the kinetic and thermodynamic parameters of the ligand exchange process between (^{tBu}POCOP)Ir(PPh$_3$) and L (L = MeCN or pyridine) were determined by employing NMR, UV−vis spectroscopy, and density functional theory (DFT) calculations to measure the relevant equilibria. A discussion of these results allows us to address whether phosphine displacement occurs via an associative or a dissociative pathway.

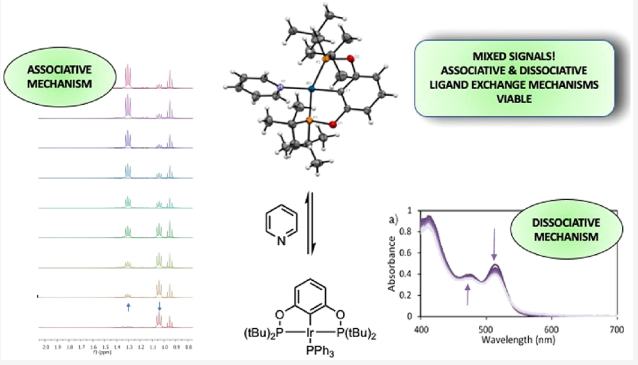

INTRODUCTION

Group 9 metal−pincer complexes of general formula [(pincer)−M(L)] (L = weakly bound ligand) can be used to prepare reactive 14-electron species, which are widely applied in a variety of catalytic transformations.[1,2] Among the numerous available ligand backbones known to support iridium−pincer complexes, POCOP has received sustained interest arising from both facile and highly modular syntheses.[3−9] Moreover, the iridium complexes of POCOP ligands have found application in numerous catalytic transformations.[2,10−16]

As a fundamental transformation in coordination/catalysis chemistry, the displacement of labile donor ligands from iridium and other metal centers has been studied by many groups. In 1976, Garrou and Hartwell reported an intermolecular ligand exchange between a halide, CO, and organophosphine ligand in the four-coordinate M(CO)(X)L$_2$ [M = Rh, Ir; X = Cl, Br; L = PPh$_3$ and others] complexes. It was proposed that exchange between CO and X occurs via a four-center associative process while the organophosphine exchange takes place through a dissociative pathway.[17] Later, Atwood described a ligand-exchange process between the *trans*-Ir(CO)L$_2$X (L = P(*p*-tolyl)$_3$ and PMePh$_2$, X = Cl, Me, or OMe). Three species were observed: *trans*-Ir(CO)(P(*p*-tolyl)$_3$)$_2$X, *trans*-Ir(CO)(PMePh$_2$)$_2$X, and *trans*-Ir(CO)(PMePh$_2$)(P(*p*-tolyl)$_3$)X upon reaction between *trans*-Ir(CO)(P(*p*-tolyl)$_3$)$_2$X and *trans*-Ir(CO)(PMePh$_2$)$_2$X.[18] The Oro group prepared cationic iridium complexes, [IrClH(P^{i}Pr$_3$)(NCCH$_3$)$_3$]BF$_4$ and [IrH$_2$(P^{i}Pr$_3$)(NCCH$_3$)$_3$]BF$_4$, and studied the rates of exchange between free and bound acetonitrile using NMR spectroscopy. Oro and co-workers proposed fluxional five-coordinate intermediates to be involved in this exchange, arising from dissociation of one acetonitrile ligand trans to hydride in both complexes.[19]

Milstein and co-workers reported an exchange study at a ^{Pyr}PCP-based rhodium(I) center. It was demonstrated that treatment of either Rh^I(^{Pyr}PCP)PPh$_3$ or Rh^I(^{Pyr}PCP)PPyr$_3$ (Pyr = pyrrolyl, NC$_4$H$_4$) with an equivalent of PPyd$_3$ (Pyd = pyrrolydinyl, NC$_4$H$_8$) led to the formation of Rh^I(^{Pyr}PCP)PPyd$_3$ with release of either PPh$_3$ or PPyr$_3$, respectively. However, addition of either 1 equiv of PPyr$_3$ to Rh^I(^{Pyr}PCP)PPh$_3$ or 1 equiv of PPh$_3$ to Rh^I(^{Pyr}PCP)PPyr$_3$ afforded an equilibrium between two complexes, shifted toward formation of Rh^I(^{Pyr}PCP)PPyr$_3$ at 295 K.[20] One year later, the Brookhart group demonstrated ligand interchange of N$_2$ with small molecules (CO, NH$_3$, C$_2$H$_4$, H$_2$, and O$_2$) could occur within

Received: March 25, 2020

single crystals of the POCOP−Ir(I)−(N_2) complex. Significantly, an associative mechanism was observed, and exchange occurred with no apparent loss of crystallinity.[21] Later, Weller and co-workers prepared a series of cationic [(PNP^R)Rh-(PCy_3)]$^+$ (R = Ph, Cy, Mes, ^{t}Bu; Mes =2,4,6-$Me_3C_6H_2$) complexes and studied the displacement of the PCy_3 ligand from the rhodium center by using CO, CH_2CH_2, MeCN, acetone, H_2, and N_2, resulting in a suite of new Rh(I)−pincer complexes.[1] In a related study, Fujita's group reported on the equilibrium and kinetics of the coordination of several small molecules (N_2, H_2, D_2, and C_2H_4) to PCP rhodium(I) complexes in different organic solvents by a combination of kinetic flash photolysis methods, NMR equilibrium studies, and density functional theory (DFT) calculations.[22] In 2015, the Zargarian research group synthesized a range of nickel−pincer complexes of type [(R-POCOP$^{R'}$)Ni(NCMe)]-[OSO_2CF_3] and investigated the effect of R and R′ groups on equilibrium constants for ligand exchange reactions in both ionic and neutral bromo complexes. It was shown that nickel-bound acetonitrile can be easily displaced by bromide and triflate anions, especially for the more electrophilic (cationic) Ni center.[23]

More recently, the MacLachlan group synthesized a square-planar pincer macrocyclic palladium complex and its corresponding open form, in which the palladium center is coordinated to a tridentate, NNN pincer bis(amido)pyridine and the final coordination site is occupied by an acetonitrile ligand. Acetonitrile exchange was studied by using six different ligands in which kinetic studies revealed that ligand substitution follows an associative pathway. Thus, an increase in steric bulk near the palladium center could prevent the ligand exchange reaction.[24]

Surprisingly, given their popularity in organometallic chemistry, to the best of our knowledge there is still a lack of comparable ligand exchange studies employing iridium−pincer complexes.[21] Previously, we have reported the synthesis of (^{tBu}POCOP)Ir(L) (L = MeCN (**2**), pyridine (**3**)) complexes (Scheme 1 and Figure 1),[25] which we viewed as

Scheme 1. Synthesis of Complexes 2−4

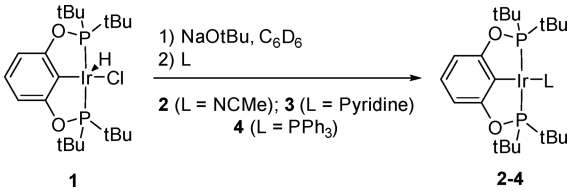

1 2-4

excellent test beds for such fundamental ligand exchange studies. Herein, we report on our experimental and computational studies of ligand exchange chemistry between (^{tBu}POCOP)Ir(PPh_3) (**4**) and exogenous ligand, L (L = MeCN, pyridine).

RESULTS AND DISCUSSION

Crystal Structures of Complexes 2 and 3. Gratifyingly, we were able to grow single crystals of complexes **2** and **3** suitable for study employing X-ray diffraction crystallography from cold (−30 °C) solutions of the complexes in methylene chloride/pentane. The solid-state structures of **2** and **3** are shown in Figure 1. The molecular structures confirm that both acetonitrile and pyridine ligands are bound to iridium through the nitrogen atom which, in both cases, is longer than the Ir−

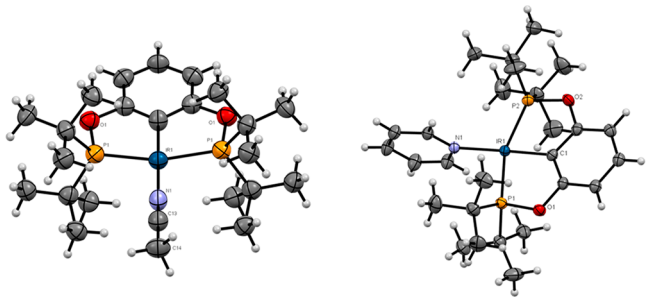

Figure 1. ORTEP diagram of (^{tBu}POCOP)Ir(NCMe) (**2**) and (^{tBu}POCOP)Ir(Py) (**3**). The thermal ellipsoids are shown at 50% probability. Carbon, hydrogen, nitrogen, oxygen, phosphorus, and iridium atoms are represented by gray, white, light blue, red, light orange, and magenta ellipsoids, respectively.

C_{ipso} bond. The compressed P−Ir−P angles of 159° for both complexes (vs 180° expected for square-planar geometry) are presumably due to steric influences arising from the bulky *tert*-butylphosphine substituents. Moreover, the C−Ir−P angle of 79° and N−Ir−P angles of 100° and 101° for complexes **2** and **3**, respectively, are consistent with a distorted square-planar geometry around the iridium center. This unsymmetrical binding motif and ligand distortion are consistent with previously published metal−pincer complexes.[1,25,26]

Ligand-Exchange Studies by NMR and UV−Vis Spectroscopy. Previously,[25] we demonstrated that addition of CO or C_2H_4 to **4** resulted in the formation of the known complexes (^{tBu}POCOP)Ir(CO) (**5**)[27] and (^{tBu}POCOP)Ir-(C_2H_4) (**6**)[28] at room temperature and 75 °C, respectively, and 1 equiv of free PPh_3.[25] In the present work, we attempted to displace PPh_3 with both acetonitrile and pyridine under ambient conditions. However, no reaction was observed even after addition of 2 equiv of exogenous Lewis base and extended reaction times (∼1 week). Subsequently, we decided to warm the reaction mixtures to 75 °C, which led to the generation of an equilibrium mixture of **4** with **2** or **4** with **3**, respectively. These results suggested, somewhat to our surprise, that coordination of CO and CH_2CH_2 to the iridium center is thermodynamically more favored than coordination of either MeCN or pyridine. With these results in hand, we further studied the exchange of PPh_3 by pyridine or MeCN at differing concentration of incoming ligand in an effort to more fully understand the underlying ligand substitution mechanism. The exchange of phosphine can occur via dissociative or associative pathways. Thus, to gain insight into the mechanism of the ligand substitution, NMR studies were performed to evaluate the effects of concentration on the equilibrium and the time required to reach equilibrium (Figure 2). Upon using 2 equiv of either acetonitrile or pyridine at 75 °C, we observed the formation of a mixture of **4**:**2**/**3** in a 1:1 ratio after the reaction reached equilibrium. Increasing the amount of added base to 4, 8, and 16 equiv shifted the equilibrium to the product side and afforded mixtures of complex **4** with either complex **3** or **2** in a 1:2, 1:4, or 1:8 ratio, respectively (Scheme 2 and Figure 2).

From our in situ NMR measurements, the kinetic profile of the displacement of PPh_3 with MeCN or Py was generated by plotting the initial rate of product formation versus concentration of exogenous base; the reaction is clearly dependent on the concentration of Py or MeCN but appears to be less than first order (Figure 3). Because changing the concentration of pyridine or MeCN shows an increase in initial

https://dx.doi.org/10.1021/acs.organomet.0c00202
Organometallics XXXX, XXX, XXX−XXX

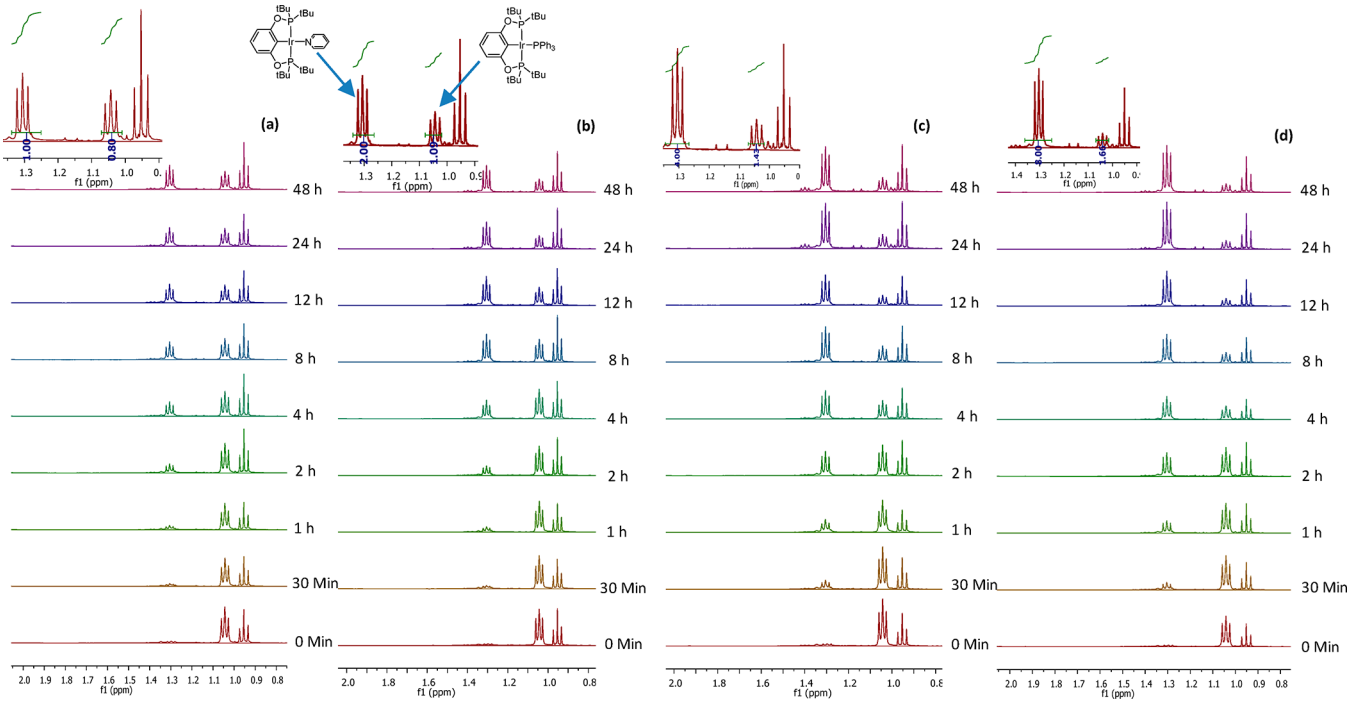

Figure 2. Stacked ^{1}H NMR spectra of (a) (^{tBu}POCOP)Ir(PPh$_3$) and (^{tBu}POCOP)Ir(Py) at 75 °C obtained in situ by addition of 2 equiv of pyridine in toluene-d_8, (b) (^{tBu}POCOP)Ir(PPh$_3$) and (^{tBu}POCOP)Ir(Py) at 75 °C obtained in situ by addition of 4 equiv of pyridine in toluene-d_8, (c) (^{tBu}POCOP)Ir(PPh$_3$) and (^{tBu}POCOP)Ir(Py) at 75 °C obtained in situ by addition of 8 equiv of pyridine in toluene-d_8, and (d) (^{tBu}POCOP)Ir(PPh$_3$) and (^{tBu}POCOP)Ir(Py) at 75 °C obtained in situ by addition of 16 equiv of pyridine in toluene-d_8. ^{31}P and ^{1}H NMR spectra for displacement of PPh$_3$ with MeCN shown in the Supporting Information.

Scheme 2. Displacement of PPh$_3$ by Pyridine and Acetonitrile

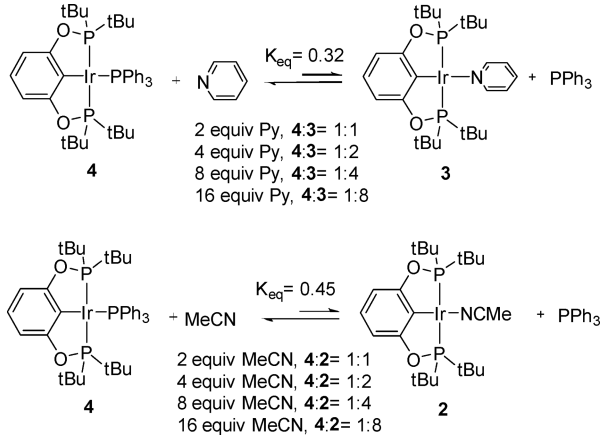

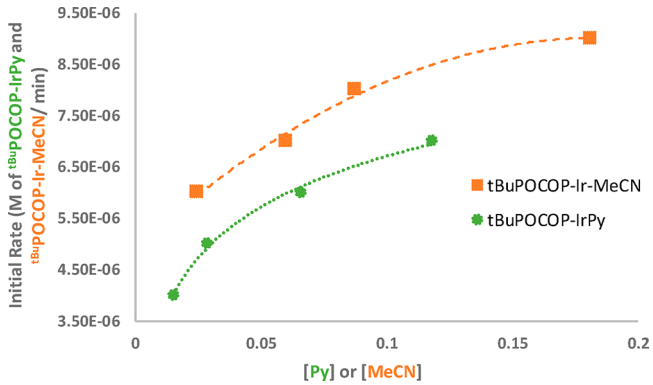

Figure 3. Plots of (a)[Py] and (b) [MeCN] vs reaction rate ($K_{initial}$); the reaction follows first-order dependence on [Py] and [MeCN]. The dotted lines are added solely as a visual aid. Equilibrium profiles for all reactions are given as Supporting Information.

rate of reaction, this strongly implies that the rate of the reaction is dependent on concentration of added ligand; hence, the substitution displays characteristics of an associative pathway.[20] To provide further support that an associative mechanism is at play, the displacement of PPh$_3$ was attempted by using sterically encumbered 2,6-lutidine (Scheme 3). In this case, even after prolonged reaction times, no phosphine displacement was observed. We attribute this lack of reactivity to the increase in steric hindrance, arising from methyl substitution in the *ortho*-positions of 2,6-lutidine which would preclude an associative pathway. Furthermore, we probed the effects of addition of free phosphine on the position of the equilibrium (Scheme 3). Addition of excess PPh$_3$ shifted the equilibrium to the reactant side, confirming the presence of an equilibrium.

Based upon the NMR spectroscopic data for complexes **2**–**4**, the coordination environment around the iridium center is consistent with pseudo-square-planar geometry with time-averaged C_{2v} symmetry.[25] The associative mechanism is considered to be more common in 16*e*, d^8 square-planar complexes and is more likely to occur for electron-deficient metal centers; this mechanism therefore avoids formation of electron-deficient 14*e* species.[20] However, in 2002, Goldman and co-workers, showed that because of repulsive interactions between the HOMO of the complex and the HOMO of an incoming ligand in square-planar d^8 ML$_4$ iridium complexes, the addition of a fifth ligand is not favored.[29] Previous

https://dx.doi.org/10.1021/acs.organomet.0c00202
Organometallics XXXX, XXX, XXX−XXX

Scheme 3. Displacement of PPh_3 by 2,6-Lutidine

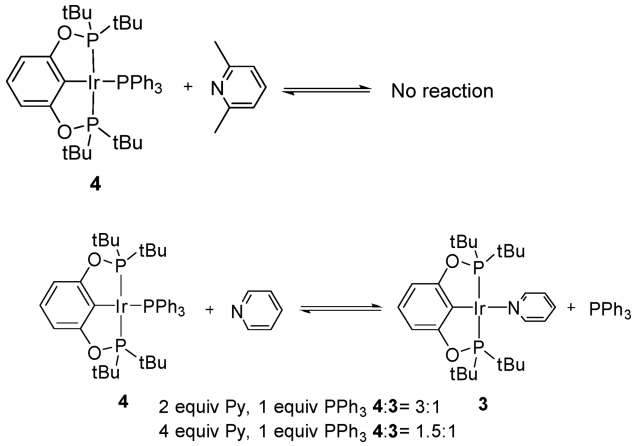

theoretical studies by the Hoffmann group revealed that the addition of a fifth ligand can happen if it occurs through a bent ML_4 geometry.[30] Moreover, this effect will be enhanced by the presence of π-accepting ligands which facilitate the coordination of the fifth ligand.[26]

Equilibrium Parameters Calculation. To measure the equilibrium constant and Gibbs free energy (eq 1) experimentally, the concentrations of complexes **3** and **4** were measured by ^{1}H NMR spectroscopy with tetraethylsilane as an internal standard (Table S1) when the reactions reach equilibrium (24 h). Knowing the total concentration of starting complex and added ligands, the relative concentrations of free ligands (Py, MeCN) were also measured. The average equilibrium constant value when Py is used as incoming ligand is determined to be 0.32 and 0.45 in the case of MeCN as incoming ligand. It should be noted that the free energy change of the reaction is equivalent to the difference in the free energies of binding of the incoming ligand Py/MeCN and the PPh_3 ligand to POCOP−Ir−PPh_3.[22]

$$K_{eq} = [\text{POCOPIr(L)}][PPh_3]/[\text{POCOP–Ir}(PPh_3)][L] \quad (1)$$

Finally, the reverse reaction, displacement of pyridine and acetonitrile with PPh_3, was investigated by using 1 equiv of PPh_3 in combination with either complex **2** or **3** (Scheme 4). The K_{eq} values for displacement of pyridine or acetonitrile with PPh_3 are both >1 and are therefore fully consistent with the conclusion that addition of PPh_3 to POCOP−Ir−L (L = MeCN or Py) is thermodynamically favored.

Scheme 4. Displacement of Py/$NCCH_3$ by PPh_3

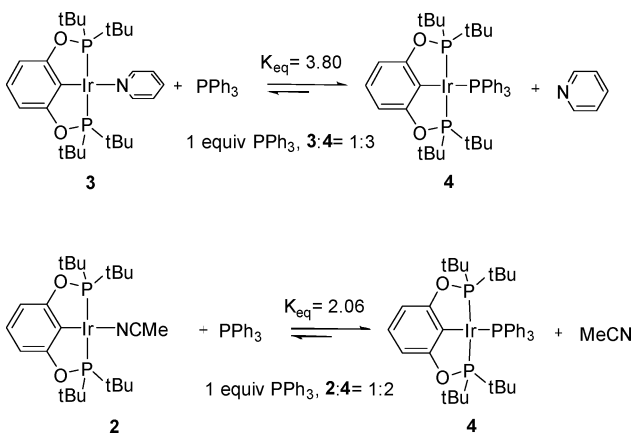

DFT Calculations. DFT calculations (PBE, ZORA, CPCM) were performed to gain insight into the reaction mechanism for the ligand exchange reaction with **4**. The geometric parameters of the optimized structures were compared with the experimentally determined values.[31] The geometry of the coordination sphere was well-reproduced, with bond distances within 0.04 Å and bond angles within 1° (Table S2) by using the TZVP basis set. Frequency calculations confirmed that the structures are energetic minima and allowed for the calculation of free energies. The Gibbs free energy values for the replacement of triphenylphosphine with acetonitrile or pyridine were calculated to be 5.8 and 3.3 kcal mol^{-1}, respectively. These values suggest that acetonitrile binding is more favorable than pyridine, and this is consistent with the relative ordering of the binding constants obtained from the solution NMR study, although the absolute values appear to underestimate the free energy of the product. To elucidate the mechanism, both associative and dissociative pathways were explored (Scheme 5). The dissociative pathway was modeled by elongating the Ir−$P_{phosphine}$ distance. The energy reached a maximum upon complete dissociation to give three coordinated iridium (path I), the presumed transition state for this pathway. The free energy barrier for this pathway is estimated as 42.2 kcal mol^{-1}, too high to proceed at room temperature.

An associative mechanism is more complicated to model as various angles of approach can be considered. Furthermore, an isomerization step is necessary, so the reaction can proceed by association, then isomerization or isomerization, and then association. Following pathway II, the ligand was stepped in at a right angle to the CP_2IrP plane to give a pseudo-square-pyramidal geometry. It was found that this pathway encounters a reaction barrier of 50.2 kcal mol^{-1}, effectively ruling it out as a viable alternative to a dissociative pathway. Assuming that both ligands follow the same mechanism, we also ruled out this pathway for the acetonitrile ligand. Considering an isomerization-first pathway (path III), the potential energy surface for the isomerization of the C−Ir−$P_{phosphine}$ bond from 170° to 90° was mapped. A potential energy surface was then mapped out by varying the Ir−N and Ir−P distances while fixing the C(39)−Ir(1)−P(3) angle at 120°. A transition state search was performed starting near the saddle point on this surface, and a geometry with a single imaginary vibrational mode was found. This transition state occurred at a calculated energy barrier (Figure S10) of 26.04 and 20.95 kcal mol^{-1} for pyridine and acetonitrile, respectively. These barriers, which are less than that calculated for the dissociative pathway, appear to support the ligand exchange occurring through an associative mechanism.

Ligand-Exchange Studies by UV−Vis Spectroscopy. It proved possible to also monitor ligand exchange processes employing UV−vis spectroscopy. The changes observed in the UV−vis spectra were monitored as a function of time while varying the temperatures (65, 75, or 85 °C) and concentrations of pyridine or acetonitrile. Figure 4 represents the changes observed in absorbance as the pyridine or acetonitrile reacts with **4** in toluene. The change in absorbance at ~515.505 nm was found to be the greatest in both reactions and was chosen as a wavelength to monitor to evaluate the kinetics. The molar absorptivity values (Figure S38) of 1670, 492, and 450 M^{-1} cm^{-1} were acquired for **4**, **2**, and **3**,

https://dx.doi.org/10.1021/acs.organomet.0c00202
Organometallics XXXX, XXX, XXX−XXX

Scheme 5. Possible Pathways for Ligand Exchange Reactions

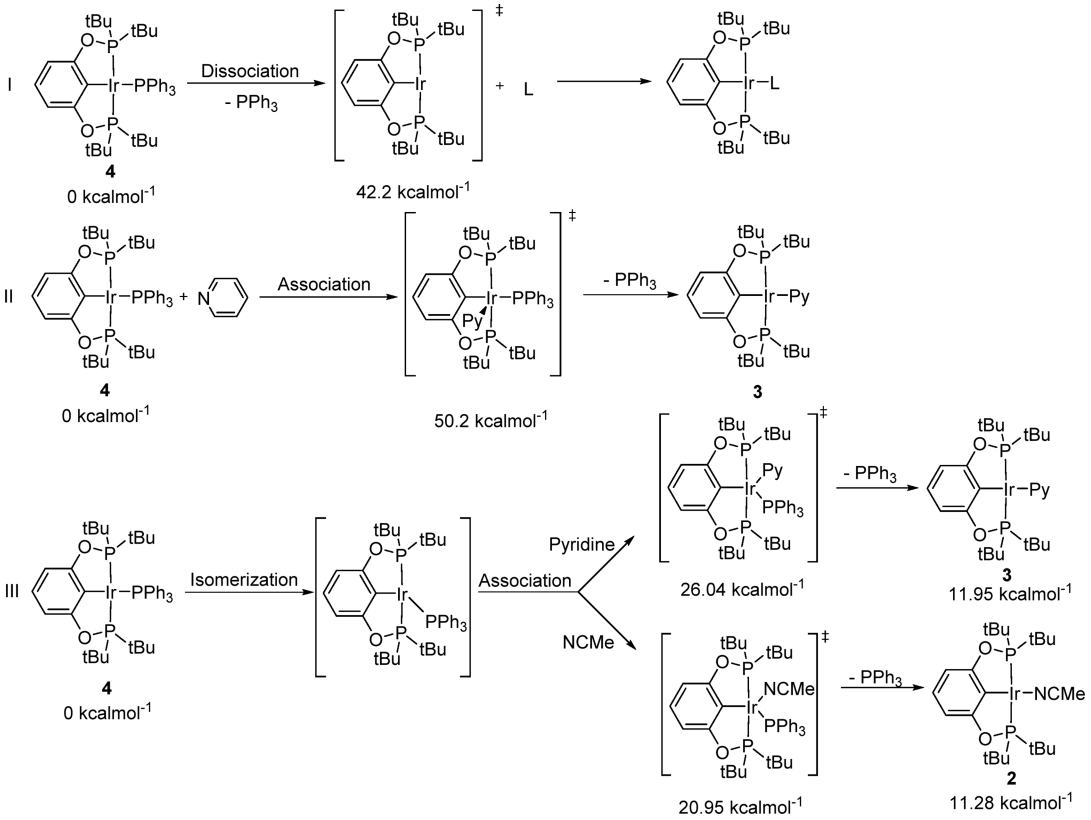

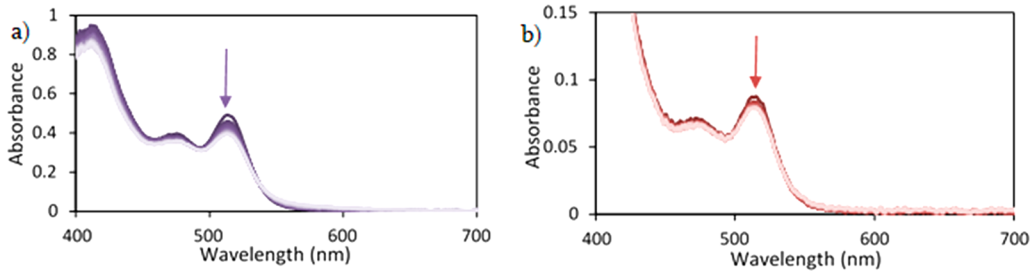

Figure 4. Plot of change in absorption with (a) pyridine and (b) acetonitrile as exogenous ligand.

respectively. Both the DFT calculations and the absence of an observable exchange reaction with lutidine (discussed previously) were consistent with an associative mechanism. However, when a solution of **4** was heated in toluene and monitored by UV−vis spectroscopy, it became clear that phosphine ligand dissociation from **4** was occurring even in the absence of exogenous ligand, strongly indicating the presence of a dissociative mechanism (Figure S47). Notably, the intensity increased toward the original value once the heating was turned off, suggesting a return to the original complex **4**. Given the apparently conflicting results, we opted to fit the ligand exchange data with two models: (1) dissociative (first order in complex concentration with forward and reverse rate constants) and (2) associative (first order in all species with forward and reverse rate constants, Supporting Information section S16). Fitting the data by using the first kinetic model resulted in different initial rates being obtained, and overall this model provided a poor fit for the data (Figure S46). Fitting the data with the second kinetic model lead to a better fit, but with some residual negative dependence on the concentration of incoming ligands. The inability to obtain a perfect fit with either model leads us to believe that at elevated temperatures it is possible to access both associative and dissociative pathways. The rate constants from the second kinetic model obtained by fitting the data at three different temperatures (Table S5) afforded a linear Eyring plot (Figure S45), and a Gibbs free energy of activation of 24.5 and 24.0 kcal mol^{-1} was determined for pyridine and acetonitrile, respectively. The entropy of activation was determined to be positive which is consistent with a dissociative process. We attribute the seemingly at odds positive enthalpy of activation and exogenous ligand dependence in the rate law to a mixture of associative and dissociative pathways being accessible under these conditions. This sheds some light on the disparate results from the previously reported CO and C_2H_4 exchange with PPh_3. The ability of CO to displace PPh_3 at room temperature suggests that the small size and high nucleophilicity of the CO allow for an associative pathway. Heating is required for the replacement of PPh_3 with C_2H_4. This suggests that a higher energy dissociative pathway needs to be accessed in order for the exchange to take place.

https://dx.doi.org/10.1021/acs.organomet.0c00202
Organometallics XXXX, XXX, XXX−XXX

CONCLUSION

We have conducted equilibrium and kinetic studies for the ligand exchange of pyridine and acetonitrile with triphenylphosphine from complex **4** by NMR and UV−vis spectroscopy. The equilibrium (NMR) and DFT studies are consistent with an associative mechanism for the displacement of PPh_3 by these ligands, but reaction kinetics as monitored by UV−vis spectroscopy revealed that both associative and dissociative mechanisms are viable and likely taking place.

EXPERIMENTAL SECTION

General Considerations. All manipulations were performed by using standard Schlenk, high-vacuum, and glovebox techniques. Argon was purified by passage through columns of BASF R3-11 (chemalog) and 4 Å molecular sieves. Anhydrous benzene and toluene were purchased from Sigma-Aldrich. Proton and carbon nuclear magnetic resonance spectra (^{1}H NMR and ^{13}C NMR spectra) were recorded on a Jeol 400 MHz spectrometer with Me_4Si or solvent resonance as the internal standard (^{1}H NMR, Me_4Si at 0 ppm, $CHCl_3$ at 7.24 ppm; ^{13}C NMR, Me_4Si at 0 ppm, $CDCl_3$ at 77.0 ppm). The relaxation delay time was set to 5 s, and the initial wait was 1 s in ^{1}H NMR of all the equilibria. All reagents, unless otherwise noted, were purchased from commercial vendors and used without further purification. The syntheses of the phosphinite complexes, (^{tBu}POCOP)Ir(H)(Cl)[27] and (^{tBu}POCOP)Ir(PPh_3),[31] have been previously described in the literature.

Computational Methods. Density functional theory (DFT) calculations were performed by using the ORCA 4.1.0 quantum chemistry program package from the development team at the Max Planck Institute for Bioinorganic Chemistry.[32] All calculations were performed by using the exchange correlation functional proposed by Perdew, Becke, and Ernzerhof (PBE)[33] with the zeroth-order regular approximation (ZORA).[34,35] Spin-restricted Kohn−Sham determinants were chosen to describe the closed shell wave functions, employing the RI approximation and the tight SCF convergence criteria provided by ORCA.[36] The atom-pairwise dispersion correction with the Becke−Johnson damping scheme (D3) were utilized for all calculations,[37,38] and the def2-SVP, def2-TZVP, and SARC/J auxiliary basis sets were used for all atoms.[39−43] The effect of solvent were also included by employing the conductor-like polarizable continuum model (C-PCM).[44] The energetics were calculated by the equation

$$\Delta G = \Delta H - T\Delta S + \mathrm{ZPE} + \mathrm{BSSE} + \Delta E_{\mathrm{solv}}$$

The ZPE is the zero-point energy, BSSE is the basis-set superposition error which was evaluated by the method given by Boys and Bernardi,[45] and ΔE_{solv} is the energy change associated with the C-PCM calculation. Analytical frequency calculations were performed on all low-energy conformations and revealed no negative frequencies. The entropy, ZPE, and BSSE values obtained from the gas-phase calculations were used for all reported values.

UV−Vis Kinetics. The control experiments were run where we heated the (^{tBu}POCOP)Ir(PPh_3) complex in toluene for the duration of kinetic experiments at 75 and 85 °C to observe any background reactivity or changes. At the end of the time heat was turned off to reduce temperature back to 25 °C, and subsequent changes were monitored (Figure S47). To study the kinetics of ligand exchange, stock solutions of (^{tBu}POCOP)Ir(PPh_3) (0.020 M), pyridine (5.00 M), and acetonitrile (5.00 M) were prepared. The exchange was monitored at three different temperatures with three (100, 200, and 300) equivalents of ligand. Inside the glovebox, the cuvette was charged with 2.00 mL of toluene, (25.00 μL, 0.020 M) of (^{tBu}POCOP)Ir(PPh_3), and pyridine (10.00 μL, 100 equiv; 20.00 μL, 200 equiv; 30.00 μL, 300 equiv) from the prepared stock solution of 5.00 M. A similar procedure was followed for kinetic run with acetonitrile. The reaction mixture was heated to temperature (65, 75, and 85 °C) with the stirring speed of 1200 rpm. The relevant spectra(s) were recorded over the range of 400−800 nm wavelength. The wavelength of 515.505 nm was chosen as the optimal wavelength for the investigation of kinetics of reaction between (^{tBu}POCOP)-IrPPh$_3$ and incoming ligand. After the solution reached equilibrium the intensity data extracted at ∼515.505 nm was fit to a calculated intensity by varying the rate constant for the particular integrated rate law by using the solver function in Excel. From these rate constants, the Gibbs free energy of activation was determined by using the Eyring equation.

General Procedure for Synthesis of Complexes 2 and 3. A scintillation vial (volume 20 mL) was charged with [(^{tBu}POCOP)-Ir(H)(Cl)] (30 mg; 0.0479 mmol), NaO^{t}Bu (5.1 mg; 0.0527 mmol), and ∼5 mL of benzene. The mixture was stirred overnight at room temperature in an argon-filled glovebox to ensure complete removal of HCl. Subsequently, (0.0479 mmol) of ligand (acetonitrile or pyridine) was added, resulting in an instantaneous color change of the reaction mixture from red to bright brown. The solution was filtered by using a syringe filter, and the volatiles were removed in vacuo to yield a light yellow solid product.[25]

Equilibrium between (^{tBu}POCOP)Ir(PPh_3) and (^{tBu}POCOP)Ir-(Py) Using 2/4/8/16 Equiv of Pyridine. To a 0.5900 mL toluene-d_8 solution of (^{tBu}POCOP)Ir(PPh_3) (6.00 mg; 0.0070 mmol) in a J-Young tube, pyridine (1.1400 μL; 0.0141 mmol/2.3000 μL; 0.0282 mmol/4.6000 μL; 0.0563 mmol/9.1000 μL; 0.1126 mmol) and tetraethylsilane (0.5000 μL; 0.0026 mmol) as an internal standard were added. The reaction mixture heated to 75 °C and monitored by ^{1}H and ^{31}P NMR spectroscopy after mixing at RT and 1, 2, 4, 8, 12, 24, 48 h of heating. After the solution reached equilibrium, concentration of each species was measured by ^{1}H NMR spectroscopy.

Equilibrium between (^{tBu}POCOP)Ir(PPh_3) and (^{tBu}POCOP)Ir-($NCCH_3$) Using 2/4/8/16 equiv of Acetonitrile. To a 0.5900 mL toluene-d_8 solution of (^{tBu}POCOP)Ir(PPh_3) (10.00 mg; 0.0117 mmol) in a J-Young tube, acetonitrile (1.2000 μL; 0.0235 mmol/2.4500 μL; 0.0469 mmol/4.9000 μL; 0.0939 mmol/9.8000 μL; 0.1878 mmol) and tetraethylsilane (0.5000 μL; 0.0026 mmol) as an internal standard were added. The reaction mixture heated to 75 °C and monitored by ^{1}H and ^{31}P NMR spectroscopy after mixing at RT and 1, 2, 4, 8, 12, 24, and 48 h of heating. After the solution reached equilibrium, the concentration of each species was measured by ^{1}H NMR spectroscopy.

Equilibrium between (^{tBu}POCOP)Ir(PPh_3) and (^{tBu}POCOP)Ir-(2,6-Lutidine). To a 0.5980 mL toluene-d_8 solution of (^{tBu}POCOP)-Ir(PPh_3) (10.00 mg; 0.0117 mmol) in a J-Young tube, 2,6-lutidine (1.3600 μL; 0.0117 mmol) and tetraethylsilane (0.5000 μL; 0.0026 mmol) as an internal standard were added. The reaction mixture heated to 75 °C and monitored by ^{1}H and ^{31}P NMR spectroscopy after mixing at RT as well as 24 and 48 h of heating. The concentration of each species was measured by ^{1}H NMR spectroscopy.

Equilibrium between (^{tBu}POCOP)Ir(PPh_3) and (^{tBu}POCOP)Ir-(Py) using 2/4 equiv of pyridine and 1 equiv of PPh_3: To a 0.5980 mL toluene-d_8 solution of (^{tBu}POCOP)Ir(PPh_3) (6.00 mg; 0.0070 mmol) in a J-Young tube, PPh_3 (1.85 mg; 0.0070 mmol), pyridine (1.1400 μL; 0.0141 mmol/2.3000 μL; 0.0282 mmol), and tetraethylsilane (0.5000 μL; 0.0026 mmol) as an internal standard were added. The reaction mixture heated to 75 °C and monitored by ^{1}H and ^{31}P NMR spectroscopy after mixing at RT and 12, 24, and 48 h of heating. After the solution reached equilibrium, the concentration of each species was measured by ^{1}H NMR spectroscopy.

Equilibrium between (^{tBu}POCOP)Ir(Py) and (^{tBu}POCOP)Ir-(PPh_3). To a 0.5990 mL toluene-d_8 solution of (^{tBu}POCOP)Ir(Py) (5.00 mg; 0.0073 mmol) in a J-Young tube, PPh_3 (1.92 mg; 0.0073 mmol) and tetraethylsilane (0.5000 μL; 0.0026 mmol) as an internal standard were added. The reaction mixture heated to 75 °C and monitored by ^{1}H and ^{31}P NMR spectroscopy after mixing at RT as well as 24 and 48 h of heating. After the solution reached equilibrium concentration of each compound was measured by ^{1}H NMR spectroscopy.

Equilibrium between (^{tBu}POCOP)Ir($NCCH_3$) and (^{tBu}POCOP)-Ir(PPh_3). To a 0.5990 mL toluene-d_8 solution of (^{tBu}POCOP)Ir-

https://dx.doi.org/10.1021/acs.organomet.0c00202
Organometallics XXXX, XXX, XXX−XXX

(MeCN) (5.00 mg; 0.0079 mmol) in a J-Young tube, PPh_3 (2.08 mg; 0.0079 mmol) and tetraethylsilane (0.5000 μL; 0.0026 mmol) as an internal standard were added. The reaction mixture heated to 75 °C and monitored by ^1H and ^{31}P NMR spectroscopy after mixing at RT as well as 24 and 48 h of heating. After the solution reached equilibrium, the concentration of each compound was measured by ^1H NMR spectroscopy.

■ ASSOCIATED CONTENT

Supporting Information

The Supporting Information is available free of charge at https://pubs.acs.org/doi/10.1021/acs.organomet.0c00202.

Equilibrium profiles, crystallographic data, NMR spectra, and DFT calculated energies (PDF)

Accession Codes

CCDC 1987628−1987629 contain the supplementary crystallographic data for this paper. These data can be obtained free of charge via www.ccdc.cam.ac.uk/data_request/cif, or by emailing data_request@ccdc.cam.ac.uk, or by contacting The Cambridge Crystallographic Data Centre, 12 Union Road, Cambridge CB2 1EZ, UK; fax: +44 1223 336033.

■ AUTHOR INFORMATION

Corresponding Authors

Michael Findlater − *Department of Chemistry & Biochemistry, Texas Tech University, Lubbock, Texas 79409, United States;* orcid.org/0000-0003-3738-4039; Email: michael.findlater@ttu.edu

Anthony F. Cozzolino − *Department of Chemistry & Biochemistry, Texas Tech University, Lubbock, Texas 79409, United States;* orcid.org/0000-0002-1100-0829; Email: Anthony.f.cozzolino@ttu.edu

Authors

Sara Shafiei-Haghighi − *Department of Chemistry & Biochemistry, Texas Tech University, Lubbock, Texas 79409, United States*

Aneelman Brar − *Department of Chemistry & Biochemistry, Texas Tech University, Lubbock, Texas 79409, United States*

Daniel K. Unruh − *Department of Chemistry & Biochemistry, Texas Tech University, Lubbock, Texas 79409, United States;* orcid.org/0000-0002-2594-5786

Complete contact information is available at: https://pubs.acs.org/10.1021/acs.organomet.0c00202

Author Contributions

S.S.-H. and A.B. contributed equally to this work.

Notes

The authors declare no competing financial interest.

■ ACKNOWLEDGMENTS

The authors gratefully acknowledge the National Science Foundation (CHE-1554906) for financial support of this work and the High Performance Computing Center (HPCC) at Texas Tech University for providing HPC resources that have contributed to the research results reported within this paper.

■ REFERENCES

(1) Chaplin, A. B.; Weller, A. S. [Rh (NC_5H_{3-2}, 6-(CH_2PtBu_2)$_2$)(PCy_3)][$BArF_4$]: A Latent Low-Coordinate Rhodium (I) PNP Pincer Compound. *Organometallics* **2011**, *30* (16), 4466−4469.

(2) Press, L. P.; Kosanovich, A. J.; McCulloch, B. J.; Ozerov, O. V. High-turnover aromatic C−H borylation catalyzed by POCOP-type pincer complexes of iridium. *J. Am. Chem. Soc.* **2016**, *138* (30), 9487−9497.

(3) Bhattacharya, P.; Krause, J. A.; Guan, H. Iron Hydride Complexes Bearing Phosphinite-Based Pincer Ligands: Synthesis, Reactivity, and Catalytic Application in Hydrosilylation Reactions. *Organometallics* **2011**, *30* (17), 4720−4729.

(4) Bhattacharya, P.; Krause, J. A.; Guan, H. Activation of dihydrogen and silanes by cationic iron bis (phosphinite) pincer complexes. *Organometallics* **2014**, *33* (21), 6113−6121.

(5) Chen, T.; Yang, L.; Li, L.; Huang, K.-W. Homocoupling of benzyl halides catalyzed by POCOP−nickel pincer complexes. *Tetrahedron* **2012**, *68* (31), 6152−6157.

(6) Li, Y.; Krause, J. A.; Guan, H. Cobalt POCOP Pincer Complexes via Ligand C−H Bond Activation with Co_2 (CO) 8: Catalytic Activity for Hydrosilylation of Aldehydes in an Open vs a Closed System. *Organometallics* **2018**, *37* (13), 2147−2158.

(7) Morales-Espinoza, E. G.; Coronel-Garcia, R.; Valdes, H.; Reyes-Martinez, R.; German-Acacio, J. M.; Aguilar-Castillo, B. A.; Toscano, R. A.; Ortiz-Pastrana, N.; Morales-Morales, D. Synthesis, characterization and catalytic evaluation of non-symmetric Pd (II)-POCOP pincer compounds derived from 2′, 4′-Dihydroxyacetophenone. *J. Organomet. Chem.* **2018**, *867*, 155−160.

(8) Pell, C. J.; Ozerov, O. V. Catalytic dehydrogenative borylation of terminal alkynes by POCOP-supported palladium complexes. *Inorg. Chem. Front.* **2015**, *2* (8), 720−724.

(9) Timpa, S. D.; Fafard, C. M.; Herbert, D. E.; Ozerov, O. V. Catalysis of Kumada−Tamao−Corriu coupling by a (POCOP) Rh pincer complex. *Dalton Transactions* **2011**, *40* (20), 5426−5429.

(10) Morales-Morales, D. Pincer Complexes: Applications in Catalysis. *Revista de la Sociedad Química de México* **2004**, *48* (4), 338−346.

(11) Kosanovich, A. J.; Press, L. P.; Ozerov, O. V. Boryl transfer reactivity of a POCOP-supported Ir-diboryl: Reduction of CO_2 to CO and borylation of other small molecules. *J. Organomet. Chem.* **2017**, *845*, 19−24.

(12) Goldberg, J. M.; Goldberg, K. I.; Heinekey, D. M.; Burgess, S. A.; Lao, D. B.; Linehan, J. C. Detection of an Iridium−Dihydrogen Complex: A Proposed Intermediate in Ionic Hydrogenation. *J. Am. Chem. Soc.* **2017**, *139* (36), 12638−12646.

(13) Goldberg, J. M.; Berman, J. L.; Kaminsky, W.; Goldberg, K. I.; Heinekey, D. M. Oxidative addition of iodine to (tBu) $_4$ (POCOP) Ir (CO) complexes. *J. Organomet. Chem.* **2017**, *845*, 171−176.

(14) Ahmed Foskey, T. J.; Heinekey, D. M.; Goldberg, K. I. Partial deoxygenation of 1, 2-propanediol catalyzed by iridium pincer complexes. *ACS Catal.* **2012**, *2* (6), 1285−1289.

(15) Park, S.; Bézier, D.; Brookhart, M. An efficient iridium catalyst for reduction of carbon dioxide to methane with trialkylsilanes. *J. Am. Chem. Soc.* **2012**, *134* (28), 11404−11407.

(16) Park, S.; Brookhart, M. Hydrosilylation of Carbonyl-Containing Substrates Catalyzed by an Electrophilic η_1-Silane Iridium (III) Complex. *Organometallics* **2010**, *29* (22), 6057−6064.

(17) Garrou, P. E.; Hartwell, G. E. Redistribution reactions of organometallic complexes. Carbonyl, halogen, and organophosphine exchange between coordinately unsaturated rhodium (I) and iridium (I) complexes. *Inorg. Chem.* **1976**, *15* (3), 646−650.

(18) Thompson, J. S.; Atwood, J. D. Rapid intermolecular ligand exchange between square-planar iridium (I) complexes: trans-Ir (CO) L_2X (X= Cl or Me, L= P (p-tolyl) $_3$ or $PMePh_2$). *J. Am. Chem. Soc.* **1991**, *113* (19), 7429−7430.

(19) Sola, E.; Navarro, J.; López, J. A.; Lahoz, F. J.; Oro, L. A.; Werner, H. Labile hydrido complexes of iridium (III): Synthesis, dynamic behavior in solution, and reactivity toward alkenes. *Organometallics* **1999**, *18* (17), 3534−3546.

(20) Kossoy, E.; Rybtchinski, B.; Diskin-Posner, Y.; Shimon, L. J.; Leitus, G.; Milstein, D. Structure and Reactivity of Rhodium (I) Complexes Based on Electron-Withdrawing Pyrrolyl-PCP-Pincer Ligands. *Organometallics* **2009**, *28* (2), 523−533.

(21) Huang, Z.; White, P. S.; Brookhart, M. Ligand exchanges and selective catalytic hydrogenation in molecular single crystals. *Nature* **2010**, *465* (7298), 598.
(22) Doherty, M. D.; Grills, D. C.; Huang, K.-W.; Muckerman, J. T.; Polyansky, D. E.; Van Eldik, R.; Fujita, E. Kinetics and thermodynamics of small molecule binding to pincer-PCP rhodium (I) complexes. *Inorg. Chem.* **2013**, *52* (8), 4160−4172.
(23) Lapointe, S. b.; Vabre, B.; Zargarian, D. POCOP-type pincer complexes of nickel: Synthesis, characterization, and ligand exchange reactivities of new cationic acetonitrile adducts. *Organometallics* **2015**, *34* (14), 3520−3531.
(24) Carta, V.; Mehr, S. H. M.; MacLachlan, M. J. Controlling Ligand Exchange through Macrocyclization. *Inorg. Chem.* **2018**, *57* (6), 3243−3253.
(25) Shafiei-Haghighi, S.; Singer, L. M.; Tamang, S. R.; Findlater, M. Synthesis, characterization and reactivity of iridium pincer complexes. *Polyhedron* **2018**, *143*, 126−131.
(26) Kossoy, E.; Iron, M. A.; Rybtchinski, B.; Ben-David, Y.; Shimon, L. J.; Konstantinovski, L.; Martin, J. M.; Milstein, D. π-Accepting-Pincer Rhodium Complexes: An Unusual Coordination Mode of PCP-Type Systems. *Chem. - Eur. J.* **2005**, *11* (8), 2319−2326.
(27) Göttker-Schnetmann, I.; White, P. S.; Brookhart, M. Synthesis and properties of iridium bis (phosphinite) pincer complexes (p-XPCP) IrH_2,(p-XPCP) Ir (CO),(p-XPCP) Ir (H)(aryl), and {(p-XPCP) Ir}$_2$ {μ-N_2} and their relevance in alkane transfer dehydrogenation. *Organometallics* **2004**, *23* (8), 1766−1776.
(28) Goldman, A. S.; Roy, A. H.; Huang, Z.; Ahuja, R.; Schinski, W.; Brookhart, M. Catalytic alkane metathesis by tandem alkane dehydrogenation-olefin metathesis. *Science* **2006**, *312* (5771), 257−261.
(29) Krogh-Jespersen, K.; Czerw, M.; Zhu, K.; Singh, B.; Kanzelberger, M.; Darji, N.; Achord, P. D.; Renkema, K. B.; Goldman, A. S. Combined computational and experimental study of substituent effects on the thermodynamics of H_2, CO, arene, and alkane addition to iridium. *J. Am. Chem. Soc.* **2002**, *124* (36), 10797−10809.
(30) Saillard, J. Y.; Hoffmann, R. Carbon-hydrogen and hydrogen-hydrogen activation in transition metal complexes and on surfaces. *J. Am. Chem. Soc.* **1984**, *106* (7), 2006−2026.
(31) Sykes, A. C.; White, P.; Brookhart, M. Reactions of Anilines and Benzamides with a 14-Electron Iridium (I) Bis (phosphinite) Complex: N− H Oxidative Addition versus Lewis Base Coordination. *Organometallics* **2006**, *25* (7), 1664−1675.
(32) Neese, F. Orca 3.0. 3. Max Planck Institute for Bioinorganic Chemistry, Mlheim/Ruhr, Germany, 2013.
(33) Perdew, J. P.; Burke, K.; Ernzerhof, M. Generalized gradient approximation made simple. *Phys. Rev. Lett.* **1996**, *77* (18), 3865.
(34) Lenthe, E. v.; Baerends, E.-J.; Snijders, J. G. Relativistic regular two-component Hamiltonians. *J. Chem. Phys.* **1993**, *99* (6), 4597−4610.
(35) Heully, J.-L.; Lindgren, I.; Lindroth, E.; Lundqvist, S.; Martensson-Pendrill, A.-M. Diagonalisation of the Dirac Hamiltonian as a basis for a relativistic many-body procedure. *J. Phys. B: At. Mol. Phys.* **1986**, *19* (18), 2799.
(36) Kohn, W.; Sham, L. J. Self-consistent equations including exchange and correlation effects. *Phys. Rev.* **1965**, *140* (4A), A1133.
(37) Grimme, S.; Antony, J.; Ehrlich, S.; Krieg, H. A consistent and accurate ab initio parametrization of density functional dispersion correction (DFT-D) for the 94 elements H-Pu. *J. Chem. Phys.* **2010**, *132* (15), 154104.
(38) Grimme, S.; Ehrlich, S.; Goerigk, L. Effect of the damping function in dispersion corrected density functional theory. *J. Comput. Chem.* **2011**, *32* (7), 1456−1465.
(39) Weigend, F. Accurate Coulomb-fitting basis sets for H to Rn. *Phys. Chem. Chem. Phys.* **2006**, *8* (9), 1057−1065.
(40) Pantazis, D. A.; Chen, X.-Y.; Landis, C. R.; Neese, F. All-electron scalar relativistic basis sets for third-row transition metal atoms. *J. Chem. Theory Comput.* **2008**, *4* (6), 908−919.
(41) Pantazis, D. A.; Neese, F. All-electron scalar relativistic basis sets for the lanthanides. *J. Chem. Theory Comput.* **2009**, *5* (9), 2229−2238.
(42) Pantazis, D. A.; Neese, F. All-electron scalar relativistic basis sets for the actinides. *J. Chem. Theory Comput.* **2011**, *7* (3), 677−684.
(43) Pantazis, D. A.; Neese, F. All-electron scalar relativistic basis sets for the 6p elements. *Theor. Chem. Acc.* **2012**, *131* (11), 1292.
(44) Barone, V.; Cossi, M. Quantum calculation of molecular energies and energy gradients in solution by a conductor solvent model. *J. Phys. Chem. A* **1998**, *102* (11), 1995−2001.
(45) Boys, S. F.; Bernardi, F. d. The calculation of small molecular interactions by the differences of separate total energies. Some procedures with reduced errors. *Mol. Phys.* **1970**, *19* (4), 553−566.

https://dx.doi.org/10.1021/acs.organomet.0c00202
Organometallics XXXX, XXX, XXX−XXX